RESEARCH ARTICLE | JUNE 12 2025

Modeling nitric oxide diffusion and plasticity modulation in cerebellar learning

Special Collection: Bioengineering of the Brain

Alessandra Maria Trapani; Carlo Andrea Sartori ; Benedetta Gambosi ; Alessandra Pedrocchi ; Alberto Antonietti

APL Bioeng. 9, 026125 (2025)
https://doi.org/10.1063/5.0250953

Modeling nitric oxide diffusion and plasticity modulation in cerebellar learning

Cite as: APL Bioeng. **9**, 026125 (2025); doi: 10.1063/5.0250953
Submitted: 28 November 2024 · Accepted: 1 June 2025 ·
Published Online: 12 June 2025

Alessandra Maria Trapani, Carlo Andrea Sartori,[a] Benedetta Gambosi, Alessandra Pedrocchi, and Alberto Antonietti

AFFILIATIONS

Department of Electronics, Information and Bioengineering, Politecnico di Milano, Milano, Italy

Note: This paper is part of the Special Topic on Bioengineering of the Brain.
[a]**Author to whom correspondence should be addressed:** carloandrea.sartori@polimi.it

ABSTRACT

Nitric oxide (NO) is a versatile signaling molecule with significant roles in various physiological processes, including synaptic plasticity and memory formation. In the cerebellum, NO is produced by neural NO synthase and diffuses to influence synaptic changes, particularly at parallel fiber-Purkinje cell synapses. This study aims to investigate NO's role in cerebellar learning mechanisms using a biologically realistic simulation-based approach. We developed the NO Diffusion Simulator (NODS), a Python module designed to model NO production and diffusion within a cerebellar spiking neural network framework. Our simulations focus on the eye-blink classical conditioning protocol to assess the impact of NO modulation on long-term potentiation and depression at parallel fiber-Purkinje cell synapses. The results demonstrate that NO diffusion significantly affects synaptic plasticity, dynamically adjusting learning rates based on synaptic activity patterns. This metaplasticity mechanism enhances the cerebellum's capacity to prioritize relevant inputs and mitigate learning interference, selectively modulating synaptic efficacy. Our findings align with theoretical models, suggesting that NO serves as a contextual indicator, optimizing learning rates for effective motor control and adaptation to new tasks. The NODS implementation provides an efficient tool for large-scale simulations, facilitating future studies on NO dynamics in various brain regions and neurovascular coupling scenarios. By bridging the gap between molecular processes and network-level learning, this work underscores the critical role of NO in cerebellar function and offers a robust framework for exploring NO-dependent plasticity in computational neuroscience.

I. INTRODUCTION

Nitric oxide (NO) is an essential molecule ubiquitously present in the human organism and has a significant role in various processes. Physiologically, for example, it acts at the vasculature level by promoting vasodilation, while in the central nervous system (CNS) as a neurotransmitter, contributing to synaptic plasticity and brain cell communication. Pathologically, aberrant NO signaling is implicated in major disorders. In the brain, excessive NO production contributes to neurodegenerative diseases like Alzheimer's and Parkinson's by promoting oxidative stress, neuroinflammation, and neuronal damage.[1–3]

What makes NO particularly intriguing as a signaling molecule is that, unlike other neurotransmitters that act on specific receptors expressed in dedicated neurons, NO can influence a wide range of neurons through various molecular mechanisms. Its low molecular weight and high diffusion coefficient in aqueous environments allow NO to diffuse isotropically from its production site, enabling forms of cellular communication that do not rely just on anatomical connections of synaptic boutons.[1,2] NO is produced by the enzyme NO synthase (NOS), which is characterized by three isoforms: endothelial NOS (eNOS) is present in endothelial cells of the vasculature, inducible NOS (iNOS), active during inflammatory response, and neuronal NOS (nNOS) expressed by neurons in the brain.[1]

A. NO physiological role in the brain

NO is produced in the CNS by nNOS expressed in specific neuronal subtypes. It can be located in the cytoplasm for small subpopulations of GABAergic (GABA) cells or in the spine head for larger populations of excitatory neurons. nNOS is physically tethered to N-methyl-D-aspartate receptors (NMDAr), which are fundamental gates for Ca^{2+} signaling, and it starts producing NO after the $[Ca^{2+}]$ increase caused by the activation of NMDAr by glutamate. Following production and diffusion, at given concentrations, NO activates

different possible biochemical cascades.[2,4] As a result, NO acts indirectly at the cellular level by impacting neuronal excitability, synaptic transmission, and propagation of action potentials. These effects can be traced as long-term plasticity mechanisms, either potentiating (LTP) or depressing (LTD).[1,2]

Furthermore, several studies (reviewed by Hardingham, Dachtler, and Fox[5]) suggested that certain stimulation patterns of a closely packed group of neurons, containing neuronal nNOS enzyme, may generate a diffuse cloud of NO, thus acting as a volume transmitter, with a relatively large area of influence on synapses.[2,4]

Extensive research has been conducted to explore the effects of NO in many brain areas. In cortical structures, NO signaling has been identified as a crucial factor in the induction of LTP.[6–9] Furthermore, in the hippocampus, NO has been commonly observed to participate in later phases of LTP,[10] while in the thalamus, increasing NO levels resulted in the potentiation of inhibitory activity.[11] Many research studies have found proof for the presence of nNOS also in the cerebellum, both in the granular layer and the molecular layer.[12–14]

B. NO physiological role in cerebellar learning

In the molecular layer, a high number of nNOS was found in the Purkinje cell (PC) dendritic tree, meaning that the NO production happens in granule cells (GrCs), both in the granular layer at the mossy fibers (*mf*s)-GrC synapses and at parallel fibers (*pf*s)-PC synapses [Fig. 1(a)].[13,15–17] Furthermore, *pf*s-PC synapses are established as one of the main actors for motor learning in the cerebellum. Therefore, it has been of great interest to study how and where NO exerts its effects in this synapse.

Lev-Ram *et al.* and Wang *et al.* conducted separate studies demonstrating the necessity of NO in both LTD and LTP.[12,13,18] A more recent study reported a form of NO-dependent LTP induced by high-frequency bursts of activity from the *pf*s.[17] These findings suggest that heterosynaptic potentiation is pre-synaptically initiated with NO acting as a diffusible messenger. However, studying NO function *in vivo* and *in vitro* is challenging due to the difficulties in implementing experiments and measuring its highly volatile nature.[15,19] To address these challenges and gain deeper insights into NO's role, a simulation-based approach becomes indispensable.

C. Modeling NO diffusive plasticity in the cerebellum

By utilizing *in silico* simulations, we can overcome the limitations of traditional experimental methods and investigate the impact of NO in a more repeatable and controlled environment. Many researchers implemented relevant computational models regarding NO-dependent biochemical cascades in *pf*s-PC synapses to help understand effects both at single and spatially grouped synapses.[4,17,20–22] These studies demonstrate the relevance of NO signaling in exerting both LTP and LTD in the PC dendritic tree. Although they evidence an important role for NO in the cerebellum characterized by a diffusive effect, there is still a lack regarding the representation of these mechanisms in a functional learning context.[17,21]

In this work, we aim to investigate the role of NO in cerebellar learning mechanisms by employing a biologically realistic simulation-based approach. With respect to previous work, we propose a more comprehensive simulation study that incorporates NO production and diffusion models within a physiologically inspired cerebellar structure,

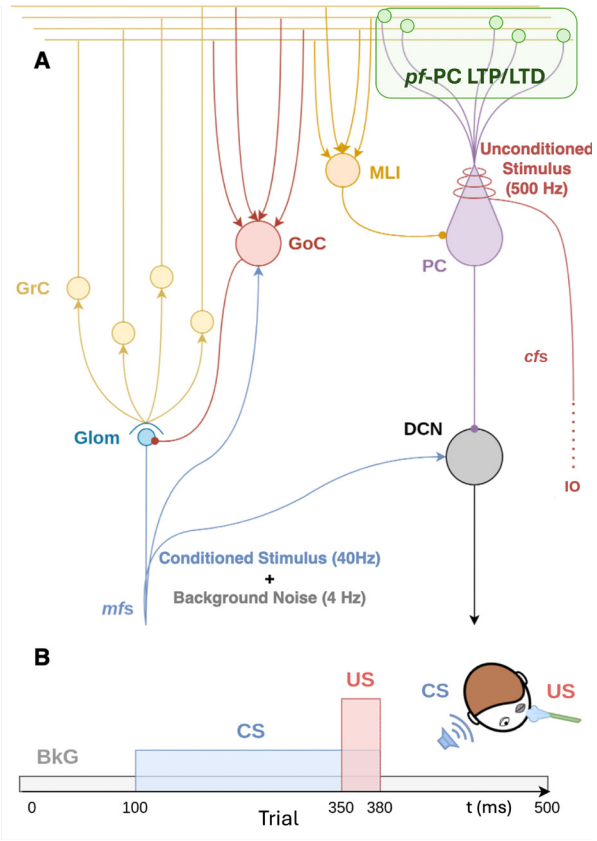

FIG. 1. Cerebellar microcircuit with plasticity domains and EBCC protocol: (a) the network is composed of mossy fibers (*mf*s), granule cells (GrCs), Golgi cells (GoCs), stellate and basket cells (SCs and BCs as MLIs), Purkinje cells (PCs), inferior olivary nuclei (IO), climbing fibers (*cf*s), and the deep cerebellar nucleus (DCN). The cerebellar circuit expresses different forms of plasticity, we focus on *pf*s-PC LTP and LTD (green area and dots in the PC dendritic tree). (b) EBCC protocol where CS and US are identified, respectively, as tone and air puff stimulus. During the time course of one trial (500 ms), *mf*s receive a background noise (e.g., at 4 Hz), whereas CS is modeled as a burst of 40 Hz spanning 280 ms, while US is conveyed as a rapid (30 ms) burst of 500 Hz to IO nuclei.

leveraging a detailed morphological and topological network.[23] We simulate a large-scale cerebellar spiking neural network (SNN) that can learn a cerebellar-driven task, namely, the eye-blinking classical conditioning (EBCC),[24] where we show the effects of NO modulation on LTP and LTD at *pf*-PC synapses.

D. Eye-blinking classical conditioning as cerebellar learning paradigm

The main functional role of the cerebellum regards motor control, where it modifies the motor commands of the descending pathways to adapt movements and increase their accuracy.[25] These modifications are due to long-term plasticity effects that allow the cerebellum to perform its motor control functions. Behaviorally, these adaptation principles of the cerebellum have been investigated using different paradigms, including the EBCC,[26,27] EBCC is one of the most studied learning models for associative learning in the cerebellum. The

standard paradigm is constituted by the repetition of a conditioned and an unconditioned stimulus (CS and US). CS is a neutral stimulus, such as a light or a tone, that does not elicit an eyelid response. It is followed by the US, usually an air puff in the cornea of the subject studied, which activates the eyelid response. The repetitive pairing of CS and US elicits an "eye-blink" conditioned response (CR), which starts during CS and anticipates the onset of US, thus predicting the incoming US by associating the two input stimuli.[26,27] Both CS and US convey sensory information to the cerebellar microcircuit through different pathways (Fig. 1). CS input starts in the pontine nuclei, which receive information from the brainstem and subcortical sources, processing auditory, visual, and somatosensory signals. This information is conveyed as CS, through *mf*s, at GrCs and Deep Cerebellar Nuclei (DCN) in the cerebellar microcircuit. In particular, CS is projected via *pf*s from GrCs to PCs. On the other hand, US input starts from the IO nuclei, receiving signals from the trigeminal nucleus, and reaches both DCNs and PCs through *cf*s.[26,27] Importantly, CS and US information arrive at PCs, the main processing unit of the circuit, which associates the incoming stimuli to produce CR. In particular, CR is codified as a depression of PC activity, which in turn increases the DCN activity, directly controlling the eyelid muscles. This learning process happens thanks to two well-known LTP and LTD plasticity mechanisms at the *pf*s-PC synapses, shaping the activity of each PC.[26,27]

In order to evaluate and better understand the functionality of the cerebellum, similarly to previous work,[24,28] we implemented an EBCC protocol with a SNN. In this paradigm, learning depends on synaptic plasticity at the *pf*s-PC level, and it has been modeled with the well-known form of supervised spike-timing dependent plasticity (STDP).[28] When a stimulus from the *pf*s precedes in a precise time window, a stimulus from the *cf*s, the weight of the *pf*s-PC synapses is depressed. In this way, in the EBCC context, the SNN predicts the incoming US by decreasing the activity only in the synapses coding for the associated CS. On the other hand, when only *pf*s stimuli are present, the synaptic weights are potentiated, which allows to control the extinction mechanism for EBCC learning.[28]

II. RESULTS

We implemented the NO Diffusion Simulator (NODS), a Python module, to simulate the NO diffusion inside a neural network that is compatible with different neural simulation environments, such as neural simulation tool (NEST)[29] and Brian,[30] and more generally with any neuronal model written in Python. The simulator takes as input the spatial coordinates ($[x, y, z]$) of the nNOS, the activity of the neurons that activate the nNOS (presynaptic spikes), and the spatial coordinates of the points where the user wants to evaluate the NO concentration ($[NO]$). The simulator output is the temporal profile of the NO signal in the evaluation points and (optionally) the temporal and spatial profile of the NO diffused from each nNOS. The simulator structure can be divided into three main blocks:

1. Geometry initialization: We compute the relative distances between all the nNOS placed in the network and all the points where the user wants to evaluate $[NO]$. Then, we link each evaluation point to the nearest nNOS within 15 μm.
2. Single source computation: For each nNOS, we simulate the spatial and temporal profile of the NO generated through a system of differential equations. The equations are presented in the *Methods* section. Then we evaluate the diffusion of $[NO]$, given by the production in every source at time $= t$, in a sphere with 15 μm radius around each nNOS.
3. Diffusion evaluation: We compute the spatial and temporal summation of the $[NO]$ provided by all nNOS surrounding each evaluation point, with respect to their relative distances, already computed in the initialization phase (first block).

NODS allows us to perform both offline simulations, where the network activity is loaded before simulating the NO production and diffusion, and online simulations, where the network activity and the NO diffusion run in parallel. In the latter configuration, for each $dt = 1$ ms of the simulated network activity, we compute the amount of NO diffused in dt.

A. Single source model

To validate the system of differential equations describing the synthesis process, we compared the results with those obtained in a different simulation environment, NEURON.[31] This simulator allows the building of detailed individual neuron properties using compartmental models. In particular, we exploited its ability to simulate, with a high level of realism, the biochemical reactions taking place in the intracellular space using the Reaction&Diffusion module in NEURON. The biochemical cascade resulting in the NO synthesis [Fig. 2(a)] has been triggered in both models by two 40 Hz burst stimuli 100 ms long, with an inter-burst interval of 300 ms. Figure 2(b) shows the spiking activity of neurons and the relative intermediate compound concentration along time, leading to NO production. The comparison between the two simulation environments expresses an almost perfect superimposition of the results. This permits the validation of the NODS model with the widely used NEURON simulation platform. Furthermore, the results show that the lower computational load production function of NODS, for NO production, is able to replicate the results of a more complex system of equations, by depending only on the time of spike events. Thus, the implementation is compatible with information encoded in a SNN as a binary time series.

Once we have obtained a reliable description of the production function, we simulated the diffusion from a single source. Figure 2(c) shows the scheme for NO diffusion in the neural network environment. Figures 2(d) and 2(e) evidence the time and space profile of the NO signal, produced by a single source stimulated with different stimulation conditions. The time profile is calculated at a distance of 200 μm, which is the average distance between the pre-synaptic side, where nNOS is produced, and the post-synaptic one, where NO-dependent reaction cascade is activated. The space profiles show a steep decrease in $[NO]$ with a concentration below 20 pM at a distance of 5 μm from the NO source, regardless of the stimulation frequency. Nevertheless, the curves show how different stimulation frequencies result in different distances covered by the NO signal. In particular, the higher the frequency, the more NO is produced, and the larger the area is covered by the NO signal. However, the model reaches a physiological saturation regarding the amount of NO that can be produced and consequently diffused between 100 and 300 Hz. We also compared the diffusion from a single source simulated with our approach with the results of Wood *et al.*,[15] where an empirical approach has been used (supplementary material Fig. 2).

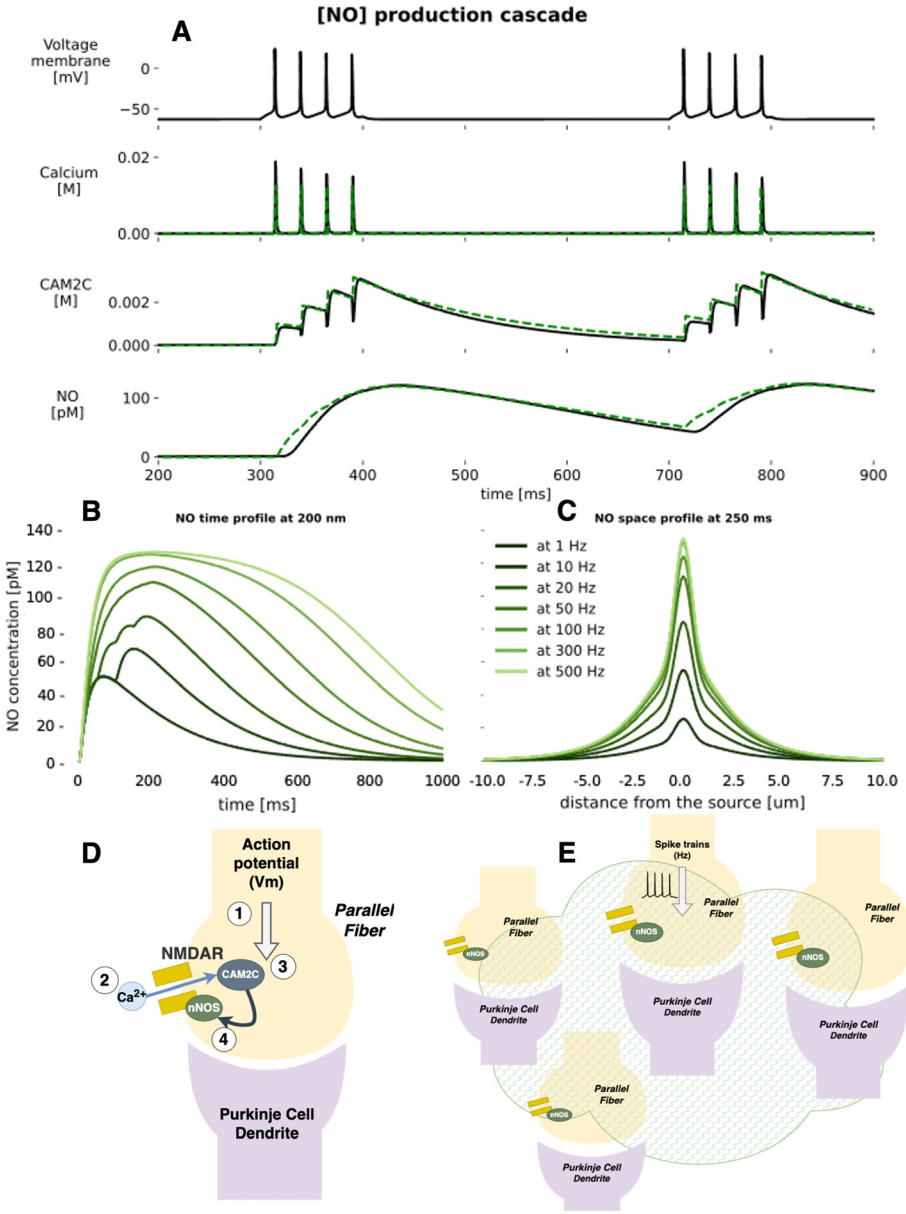

FIG. 2. Comparison of NODS and NEURON Reaction&Diffusion module: (a) [*NO*] reaction cascade characterized by instantaneous Ca^{2+} events, following spikes, causing a smooth buildup of NO. Time (b) and space (c) profile of the NO signal, produced by a single source stimulated with different frequencies (color-coded by darkening the shade of green): single spike, 10, 20, 50, 100, 300, and 500 Hz. All stimuli have been delivered at $t_i = 0$ ms and last for 200 ms. (d) Reaction cascade leading to NO production. (1) Spike train arriving at the *pf* presynaptic site leads to depolarization, which causes Ca^{2+} entrance (2) through NMDA receptors. Ca^{2+} reacts with calmodulin to form the Calm2C complex (3) that activates nNOS and thus NO production (4). (e) Scheme of NO diffusive cloud following production, where its radius (15 μm) is highlighted.

B. NO production and diffusion in EBCC simulation

We assessed NO production and diffusion in the EBCC protocol through the analysis of the variation of the NO concentration and G_{NO} during different simulations. G_{NO} is a sigmoid function that depends on [*NO*] [see Eq. (6)], and it provides a gain factor that modulates the learning rate. First, these variables were evaluated by differentiating the *pfs*-PC synapses into two groups: one comprises all synapses in the area of CS (PC-CS), which thus receive nNOS production given by CS and noise stimuli, while synapses in the other group are outside of the CS stimulation area and thus receive only noise (PC-noise). For both groups, we evaluated the mean NO concentration by averaging all the respective synapses. As NO production depends directly on spiking activity, the behavior of these groups is highly differentiable (supplementary material Fig. 3): with both CS and noise, NO concentrations oscillate due to the higher GrCs activity during CS, with a replicable increase and decrease, with the onset and the ending of the stimuli. The noise component in this case is evidenced only by some slight variations to the main oscillating trace. On the other hand, noise alone provides random activity characterized by significantly lower values of NO. By considering the threshold of 100 pM that we applied in the NO-dependent STDP rule [Eq. (6)], we characterized $G_{[NO]}$. Thus, for PC-CS synapses, we have values spanning rapidly from 0 to 1, following CS start and ending, while PC = noise synapses remain almost always equal to 0, with some slight variation when increasing the noise.

We then evaluated the same group of synapses receiving the CS with increasing noise. The NO concentration with 0 Hz remains over the threshold only during the CS window stimuli. Interestingly, when increasing the noise, NO starts building up before the CS onset and remains higher between two successive CS, proportionally to the amount of background noise. This is reflected on $G_{[NO]}$, where its value is kept closer to the maximum with increasing noise (supplementary material Fig. 4).

C. Comparison of standard and NO-dependent STDP

To test the hypothesis formulated in many experimental studies,[4,12,16] that the NO enables plasticity when relevant signals are delivered to the cerebellum, we tested and analyzed the results of two stimulation case scenarios applied to our cerebellar SNN, comparing the network activity with and without NO-dependent plasticity. The SNN is shown in Fig. 1(a) (details about neuronal models and connectivity are reported in *Methods*). In particular, after applying only background noise stimuli (0, 4, 8 Hz), we evaluate the rate of weight updates, computed as the mean number of updates for each synapse. Instead, to analyze how the learning changes upon the introduction of NO dependency, we evaluate the PC firing modulation and the subsequent influence on DCN, during complete EBCC simulations. We compare the EBCC featuring the standard STDP at three different background noise levels (0, 4, and 8 Hz) with the respective simulations that featured NO-dependent STDP [Fig. 1(b)].

1. Background noise only simulations

As reported in both modeling and experimental studies[4,5,12,21] only neighboring small groups of *pf*s activated close in time at a certain frequency would exert plasticity or, in simulation terminology, update their (synaptic) weights, due to the presence of a NO cloud produced in the area where each group is located. From the results of background noise only simulations, we observed that with NO-dependent STDP, each weight is less likely to update. In supplementary material Table 4, we report the rate of weight updates mediated for five simulations with three different noise levels. The rate is calculated by taking all the weight updates for each synapse and dividing them by the total simulation time. We then averaged for all the synapses and all the simulations. Given the hypothesis that the background noise does not correlate in a specific space of the granular layer, it activates "isolated" *pf*s, resulting in smaller NO clouds not capable of influencing neighboring synapses. Thus, these synapses will be less likely to reach the threshold value of NO required to update.

2. NO-dependent plasticity in EBCC protocol

To test the hypothesis that NO facilitates the selection and updating of synapses according to the relevance of a given context, we investigated whether its presence would increase the robustness of learning efficiency under different levels of background noise. Given the different behavior between synapses receiving CS and only noise stimuli, we maintained this division when comparing standard and NO-dependent STDP during EBCC simulations. Specifically, we split the PC cells into two populations: one receiving a high component of CS (PC-CS) and another receiving mostly noise (PC-noise) (see *Methods*).

In Figs. 3(a) and 3(b), we show the paired comparison of PC-CS population responses as spike density function (SDF) amplitude (averaged across five simulations) for 30 trials with a background noise of 4 Hz. We highlight the comparison between a network featuring standard STDP during the EBCC protocol as control [Fig. 3(a)] compared to the network featuring the NO-dependent STDP rule [Fig. 3(b)]. The main qualitative change is a lower learning effect in the network with NO plasticity. This is more evident in the baseline window, which shows a significant shrinking in the SDF traces trial-by-trial, indicating that the effect of 4 Hz noise (which would normally cause an anticipation of depression related to CR) is inhibited, and learning remains more pronounced in the CR window.

From a quantitative perspective, we evaluated an SDF-change index for the PC-CS population, calculated by subtracting from each trial's SDF values the average SDF of the first three trials. The SDF-change was calculated for both the baseline and CR windows (Fig. 3), averaged across five simulations, and compared to evaluate the amount of depression at the PC level in the simulated EBCC protocol. Figure 4 provides a comparison between standard STDP (black curves) and NO-dependent STDP (green curves) with increasing noise. At 0 Hz background noise, both baseline and CR SDF-change decrease more with standard STDP than with NO-dependent STDP [Fig. 4(a)]. With 4 Hz noise, the NO-dependent curves show only small changes, remaining stable at values similar to those at 0 Hz. In contrast, standard STDP exhibits higher depression in both baseline and CR windows due to learning at synapses activated by noise, which impairs physiological CR learning [Fig. 4(c)]. When simulating with 8 Hz, we observe comparable behavior with and without NO. This occurs because the high amount of spiking activity activates NO production and diffusion, which in turn activates plasticity already in the baseline window, thus disrupting the stabilization observed with 4 Hz noise [Fig. 4(e)].

To complete the analysis of NO-plasticity effect at the *pf*-PC synapse level, we mediated the SDF-change index for the last five trials of the baseline and CR window, of the five simulations. We evaluated the statistical differences between the standard STDP and the NO-dependent STDP EBCC performance, for both the PC-CS and PC-noise populations, by using a Wilcoxon statistical test with statistical significance at $p < 0.01$ [Figs. 4(b), 4(d), and 4(f)]. The distribution of the values highlights the same pattern of the SDF-change curves. We denote a significant statistical difference for all the paired baseline and CR window SDF-change distribution for both 0 and 4 Hz, but not for 8 Hz, in the PC-CS population. Furthermore, Fig. 4 shows the different behavior of the PC-CS and the PC-noise populations (all statistically significant at $p < 0.01$), the latter characterized by a lower SDF-change for all the background noises. Similar to the PC population, we separated the DCNs into two distinct subpopulations. After calculating the average number of PC-CS connections to each DCN, we divided the population by distinguishing those with higher vs lower numbers of connections relative to the mean (DCN-CS and DCN-noise). Figures 3(c) and 3(d) show the SDF of the DCN-CS population with and without NO, normalized by the activity of all DCNs in the baseline window. With 4 Hz noise, the DCN-CS activity with NO plasticity is qualitatively lower in the baseline window compared to the standard condition. Furthermore, with standard STDP, there is a greater increase in the baseline window, while NO builds up only with the CS, restricting learning to the CR window. To quantify the differential

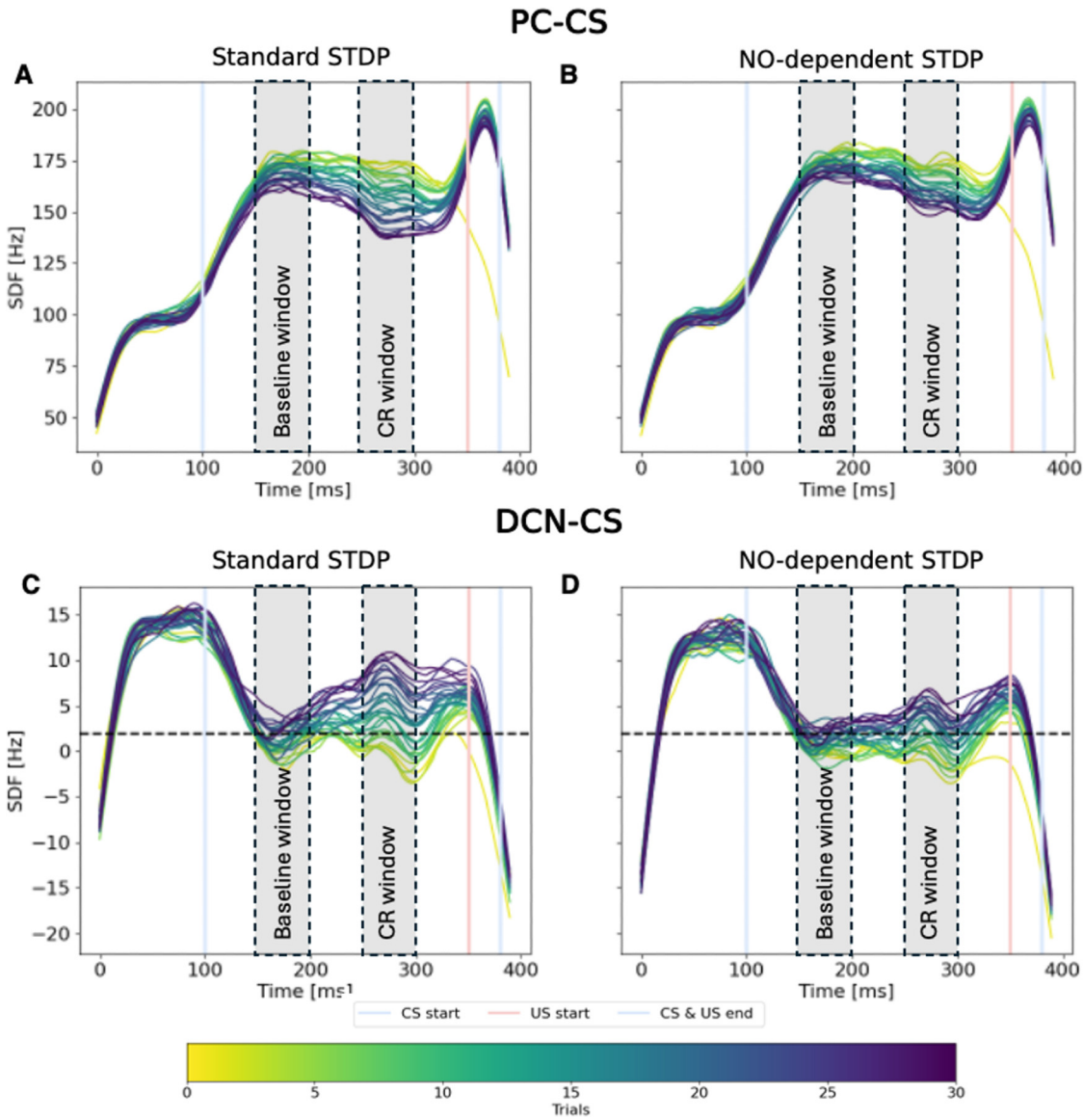

FIG. 3. Comparison of PC-CS SDF and DCN-CS SDF over trials with standard STDP and NO-dependent STDP: both panels report the SDF in PC population (averaging across cell SDFs) for each trial. The progress of the trials is color-mapped by the horizontal color bar below. The vertical lines represent the CS-onset (light blue), US-onset (light red), and CS-US co-termination (lilac). In gray are shown the two windows, baseline and CR window, for evaluation of functional plasticity. Regarding the DCN-CS SDF, the threshold for calculating the CR% is represented as a black dashed line. On panels (a) and (c), the results of EBCC are simulated using the standard STDP rule. On panels (b) and (d), the results of EBCC are simulated using the NO-dependent STDP rule. PC-CS activity shapes the DCN-CS one by inhibiting it. Thus, the depression along trials for PC-CS is reflected in a higher spiking activity for DCN-CS. Regarding network learning, the main difference between the results for the standard and the NO-dependent STDP is given by the flattening of the curve in the baseline window for both PC-CS and DCN-CS with NO.

plasticity with increasing noise, we calculated the percentage of learning during the EBCC protocol as the amount of CR% (see *Methods*). As reported in Figs. 5(a)–5(c), NO maintains more stable learning when noise increases from 0 to 4 Hz. Under 8 Hz background noise conditions, slightly faster learning occurs in the initial phase of the protocol without NO. However, by the end of the simulation, we could not distinguish any separation between the CR% curves in the two conditions.

III. DISCUSSIONS

This work is positioned in the context of modeling cerebellar learning mechanisms through the use of SNNs with the development of NO-dependent plasticity. As mentioned above, there are plenty of articles in the literature analyzing the role of the cerebellum in motor control through different learning protocols, as the EBCC,[26,27] which has also been employed in various examples of cerebellar microcircuit SNNs.[24,28] On the other hand, nitric oxide is a neurotransmitter

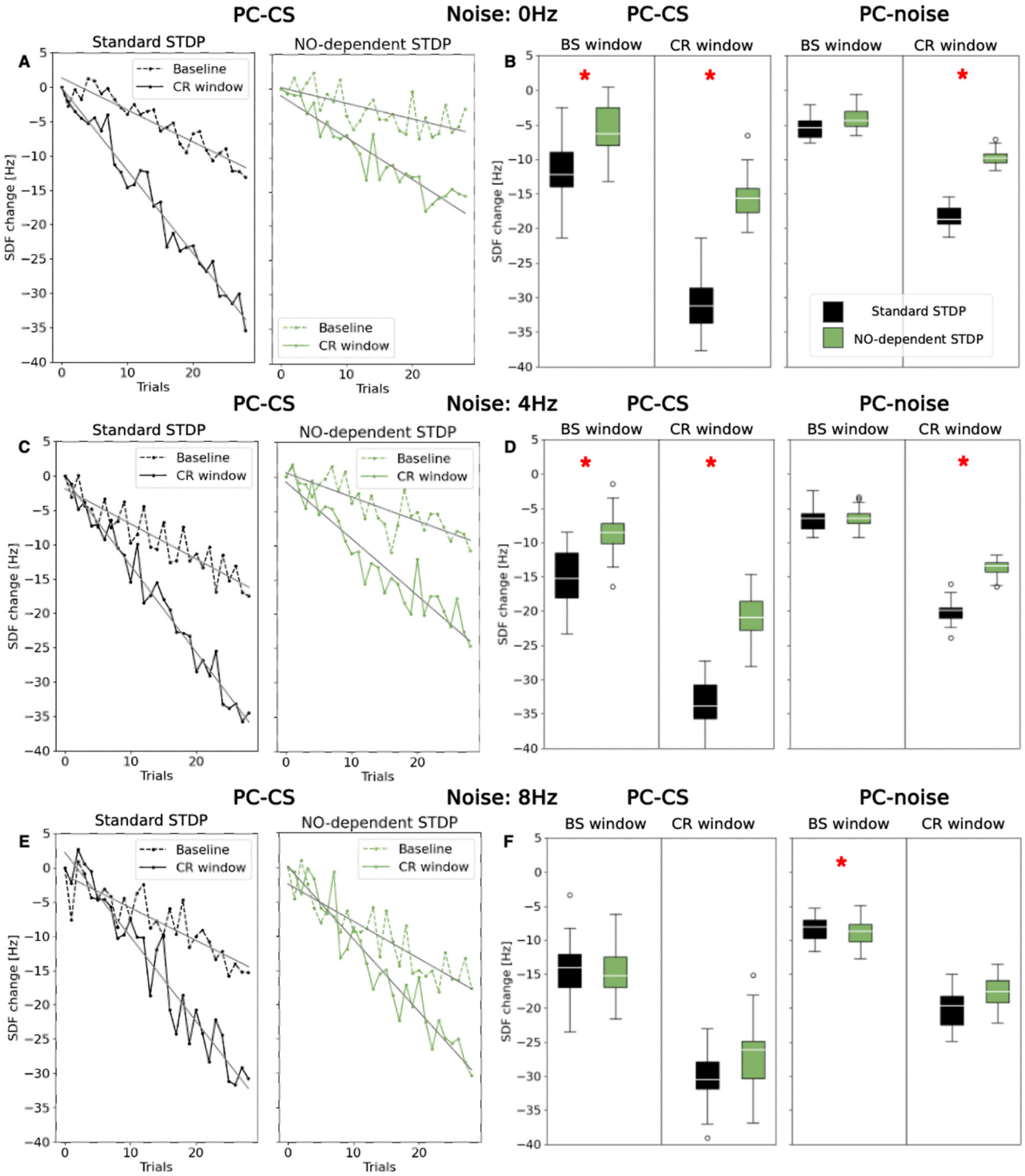

FIG. 4. SDF-change for different levels of background noise: standard STDP is color-coded in black, and NO-dependent STDP is color-coded in green. (a), (c), and (e) Dashed lines connect the SDF-change computed in the baseline window in each trial, while continuous lines connect the SDF-change computed in the CR response window. The overimposed gray lines represent the linear fitting of the SDF-change curves, which help visualize the average change during the trials. (b), (d), and (f) SDF-change in PC from the last five trials, for EBCC protocols with a background noise of 0, 4, and 8 Hz. Standard STDP is color-coded in black, and NO-dependent STDP is color-coded in green. The red $*$ corresponds to $p < 0.01$ in the Wilcoxon test.

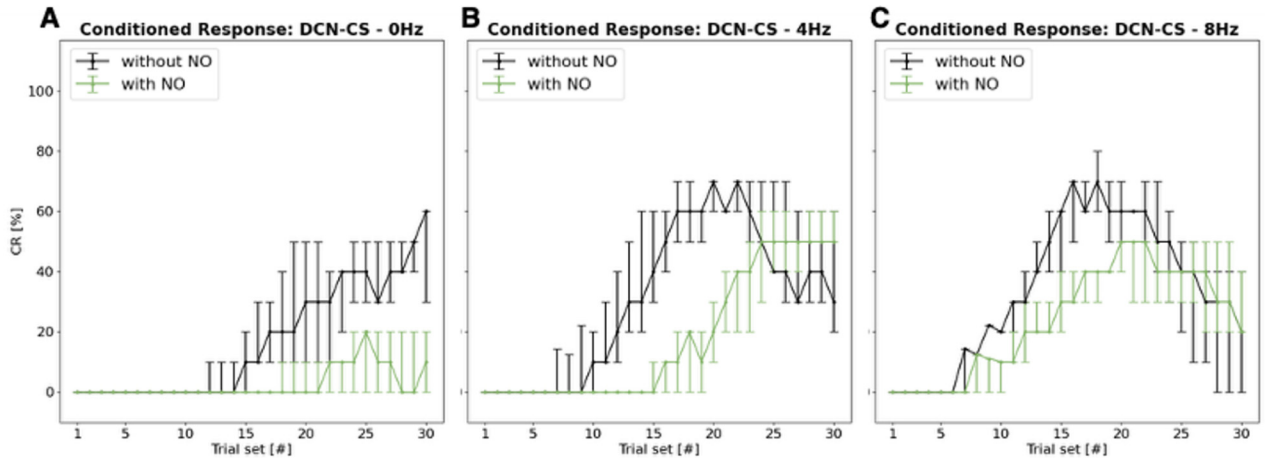

FIG. 5. CR% for different levels of background noise: standard STDP is color-coded in black, and NO-dependent STDP is color-coded in green. The curves are obtained by calculating for each trial the amount of relevant learning (as 0 or 1) and then applying a moving average (left zero-padding). Then, from the distribution of the values of each trial for the five simulations, we extracted the median value, plotted together with an error bar of the first and third quartiles.

produced in the cerebellum and capable of diffusing in the tissue and activating spatially grouped synapses around its sources.[1,2,4] In the cerebellum, the experimental investigation of NO at the *pf*s-PC synapses proves it to have a role as a necessary but not sufficient condition for both LTP and LTD.[12,13,15,18] Furthermore, there can be found in the literature simulation studies of NO-dependent plasticity at the *pf*-PC level, both at single synapses or that evaluate NO diffusive effect from one synapse to the others.[17,21] Bouvier *et al.* proposed a mechanistic model of the synapse implementing an STDP plasticity including NO. They hypothesize that the variations of calcium and nitric oxide at each postsynaptic side are driving synaptic plasticity activation and sign. Conversely, in their study, Ogasawara *et al.* integrated established models of PC electrophysiology, calcium dynamics, and signaling pathways for *pf*-PC LTD and highlighted the critical influence of local NO concentration in the induction of LTD and its impact on input specificity. They found that excessive activity in neighboring *pf*s leads to NO accumulation, resulting in LTD in synapses that were not directly stimulated, therefore compromising input specificity. Based on these findings, they propose the hypothesis that NO serves as a contextual indicator as long as a small number of *pf*s codes for a movement.[21] By taking together all these previous results, we presented a model that aims to adding NO molecular synaptic components in a geometrically plausible SNN. Through the analysis of the results of EBCC protocol learning, we wanted to assess the hypotheses of NO role in cerebellar learning and further improve its understanding.

A. Single source model and the NODS simulator

The first stage of studying the diffusive NO-dependent plasticity was to create a simulator for its production and diffusion. We successfully developed NODS, capable of generating a physiological concentration of NO upon neuronal activation through the nNOS sources and computing its spatial and temporal diffusion in all the pre-defined points of the surrounding volume. First, with this simulator, we are able to translate spiking activity in NO production at every activated synapse. Given that NODS is suited for an SNN framework, we applied some modifications to ensure a low computational load, so as to not burden the simulation time of large-scale networks, and shape NO biochemical cascade and kinetics dependently on spike trains. Although simplified, our NO production algorithm gives results in line with the ones obtained with NEURON, which are based on multicompartmental models. Altogether, this testifies to both NODS validation and its improvement with respect to state-of-the-art simulators.

Furthermore, the biochemical cascade initiated by the activation of nNOS leads to NO production and its diffusion profile. This is characterized by a rapid decay and a constrained spatial distribution, in line with[4] the production and diffusion model, which underpins the localized yet significant impact of NO on synaptic plasticity. From the point of view of NO functionality, the fine-tuned regulation ensures that NO-mediated signaling remains confined but effective, influencing synaptic efficacy and learning rates within a delimited spatial domain. The development of the production and diffusion model for a single NO source is an important starting point for understanding the role that NO plays in cerebellar plasticity. NODS model tries to replicate the biochemical and physical processes underlying NO diffusion and provides a critical link between molecular activities and synaptic changes at the network level. By simulating the spatiotemporal dynamics of NO diffusion from a single nNOS enzyme source, the model captures the balance between NO production rates, its diffusion through the neural tissue, and the eventual inactivation or consumption of NO molecules. NODS is developed to work in an SNN framework. Thus, it has to ensure a low computational load, so as not to burden the simulation time of large-scale networks. When simulating the NO signaling pathway, the geometrical organization of nNOS and the synapses in which NO is produced becomes crucial, as they determine the formation of the NO cloud and its influence on specific synapses.

B. Role of NO in the cerebellar circuitry

To investigate the impact of the NO signal on cerebellar adaptation, we modified the STDP learning rule developed to model LTP and LTD at *pf*-PC synapses.[28,32] These modifications account for the involvement of NO in the plasticity process, aiming to improve the network's adaptation in a EBCC protocol. The simulations comparing

standard and NO-dependent STDP with only background noise evidence that NO acts as a plasticity buffer, controlling the changes of synaptic weight. By evaluating these results together with the NO diffusive profile properties, we can establish its role in activating plasticity in grouped synapses with sustained activity.[21] In this context, noise-only simulations provide a basic understanding of how NO behaves under conditions of sparse spiking activity. These simulations show that random synaptic activity alone does not allow NO concentrations to build up effectively due to the nature of its production and diffusion. This is reflected in the results as a sharp drop in the synaptic weight update rates (supplementary material Table 4). To further explore NO role, we qualitatively and quantitatively analyzed network activity during simulations with EBCC. The population division based on the amount of CS arriving at PCs and DCNs helps focus on the real changes taken by NO. These would have been hidden by the background activity of the PC-noise and DCN-noise, expressing a low spiking activity and thus a low learning outcome (supplementary material Fig. 3). In the SDF of PC-CS, under 4 Hz stimulation [Figs. 3(a) and 3(b)], differences between simulations with and without NO become evident. As the number of trials increases (from yellow to purple traces), we observe reduced depression during the baseline window, while activity during the CR window remains almost similar. When these results are considered alongside the NO concentration profile during simulations with a 4 Hz CS + noise stimulus (see supplementary material Fig. 3), it becomes clear that the outcome is driven by the slow accumulation of NO in synapses during CS presentation. NO starts at low levels early in the CS onset and peaks during the CR window. To quantitatively assess NO's influence on learning at the level of the PC dendritic tree, we calculated an index of change in the SDF. This was done by subtracting the SDF value in each window (baseline and CR) of a given trial from the average SDF of the first three trials, providing a measure of learning over time. This analysis was repeated under different background noise levels (0, 4, 8 Hz), both with and without NO. What we expect from an efficient learning system tested with an EBCC protocol is to have a greater depression (absolute higher SDF-change) during the CR window with respect to the baseline window. According to the STDP rule, the LTD should be stronger between 50 and 100 ms before the US stimulus to elicit a correct anticipatory response (in our case, between 250 and 300 ms of each trial). The resulting plots of SDF-change indices reveal that learning dynamics at the PC-CS level differ depending on the presence of NO and the amount of background noise. Furthermore, following the considerations on SDF plots, the NO component has a stabilizing effect by lowering the plasticity activation in the baseline window, while keeping similar values of SDF-change index during the CR window. From a functional point of view, these results explain a double effect of NO at the *pf*-PC synapse level: by modulating NO production and diffusion in response to synaptic activity, our model demonstrates a mechanism through which the cerebellum can adjust learning rates, enhancing its capacity for rapid adaptation to new motor tasks or environmental changes. On the other hand, our findings contribute to understanding how the cerebellum addresses the potential issue of overfitting, given the vast number of synapses per Purkinje cell. NO implements a selection of inputs coming from *pf*s. This plays a crucial role in focusing learning on relevant synapses while minimizing adjustments to those less involved in the task at hand (supplementary material Fig. 3). To evaluate the specific role of NO in shaping learning outcomes during the EBCC protocol, we analyzed how changes in PC activity affect the downstream population of DCNs, and consequently, the expression of the conditioned response (CR) as the amount of CR%. Similar to our approach with PCs, we began with a qualitative analysis of DCN-CS SDF [Figs. 3(c) and 3(d)]. In this case, we applied pre-processing by normalizing DCN activity to the baseline of the first three trials within the baseline window. This normalization allowed us to track how SDFs changed across trials. We then employed a 2 Hz threshold (similar to Geminiani *et al.*) to determine whether a CR occurred. Qualitatively, we observed a change in DCN-CS activity that reflects the results of PC SDF, with an important flattening of the curves during the baseline window. On the other hand, for the quantitative analysis, we compared CR% values under different levels of background noise (0, 4, and 8 Hz), both in the presence and absence of NO-dependent plasticity. Due to the lower concentration of NO in the PC dendritic trees during 0 Hz noise [Fig. 5(a)], the CR% along with trials remains stable but slightly under the standard STDP case. Importantly, when increasing the noise to 4 Hz, the standard STDP lost its specificity of training because of the increase in activity both in the baseline and the CR window. This is reflected by a bell-shaped CR% curve, which we can associate with an irrelevant CR [Fig. 5(b)]. In the EBCC context, it results in a worse time-locked CR that is anticipated due to the association of noise with the US. The employment of NO-dependent plasticity rescues the CR timing by decreasing the DCN-PC activity in the baseline window. Thus, it stabilizes the learning outcome, and we observe a more consistent CR% curve. Functionally, this illustrates how NO-mediated plasticity mechanisms could mitigate learning interference by differentiating between relevant and irrelevant inputs.

NO diffusion serves as a gating mechanism: it associates higher learning rates with synapses experiencing temporally correlated activity with error signals and reduces the influence of synapses with less relevant input. By applying it during a motor learning functional protocol, we assess that NO plasticity contributes meaningfully to motor command learning, thereby reducing the potential for interference and enhancing the cerebellum's ability to construct accurate internal models. At last, with 8 Hz noise simulation, we have a larger component of interference on spiking, which impairs learning also with NO-dependent STDP [Fig. 5(c)].

IV. CONCLUDING REMARKS

Our research bridges the critical gap between molecular processes and network-level learning by employing a bottom-up approach that integrates NO dynamics with neural plasticity mechanisms. Through this methodology, we successfully translated molecular NO diffusion into functional STDP plasticity effects, revealing how this gaseous neurotransmitter fundamentally shapes learning in cerebellar circuits. The computational model we developed serves as a versatile tool for investigating NO's role across multiple scales of neural organization. It can be readily applied to diverse simulation scenarios, from individual neurons to extensive networks, providing a valuable resource for researchers interested in examining NO dynamics in various contexts. Our approach demonstrates how spatially distributed synaptic modifications regulated by diffusible messengers contribute to the cerebellum's capacity for learning and adaptation. By implementing NO-dependent plasticity within a cerebellar microcircuit, we have shown that varying NO concentrations significantly adjust synaptic learning rates, enabling the cerebellum to filter irrelevant inputs and enhance the fidelity of motor learning. The efficient implementation of NO

diffusion developed here offers the scientific community a flexible tool that can interface with different simulation platforms. Furthermore, a following application would be the simulation of NO-dependent plasticity in other brain areas, where its function is proven experimentally only at the single synaptic level or without the chemical cascade underneath.[10,11] This application could encourage the study and understanding of forms of functional plasticity and their relation to the geometric spatial organization of synapses. Furthermore, NODS could be employed to model neurovascular coupling by evaluating NO production and diffusion at eNOS, together with nNOS. This modeling could help elucidate the mechanisms underlying blood flow regulation in response to neural activity, contributing to a better understanding of neurovascular activity both in physiological and pathological situations.

A. Limitations and future developments

The current implementation of NODS is a flexible Python module capable of simulating NO diffusion across different network configurations. It effectively models scenarios where the spiking activity stimulates nNOS, given the coordinates of nNOS and the evaluation points for NO concentration. However, NODS implementation could be significantly improved, in terms of simulation times, by parallelizing the computation of the diffused NO from each nNOS source. Future enhancements could focus on improving NODS compatibility with simulators that do not rely exclusively on point neuron models. For example, by integrating inputs of actual Ca^{2+} concentrations that trigger NO production in compartments where nNOS is located, NODS can provide more efficient simulations of NO dynamics in complex neuronal architectures. Furthermore, given the presence of nNOS also in the granular layer and the role of NO in plasticity, it would be significant to implement the NO-dependent plasticity mechanism also at the *mf*s-GrCs synapse level. Another possible development path involves integrating NODS into larger simulations that include representations of the vascular system. This would enable the study of neurovascular coupling phenomena, necessitating the inclusion of endothelial NO synthase sources. Modifying NODS to account for endothelial NO synthase parameters will be crucial for accurately modeling NO production and diffusion in contexts where blood flow and vascular responses play significant roles in neural activity and plasticity. By pursuing these enhancements, NODS can become an even more powerful tool for researchers, facilitating comprehensive studies that span from intracellular processes to system-wide interactions.

V. METHODS

A. NODS: Nitric oxide diffusion simulator

1. Single source model

a. Production equations. The dynamics of NO production depends on a complex biochemical reaction cascade. A spike train stimulates NMDA receptors. Ca^{2+} enters the intracellular space through the NMDA receptor, increasing the intracellular concentration of Ca^{2+}. Ca^{2+} in turn binds to calmodulin, creating a calmodulin/calcium complex (Calm2C) whose concentration rises following Ca^{2+} events. This induces a catalytic activation of the nNOS enzyme that starts producing NO using oxygen and reducing NADPH to catalyze the conversion of arginine to citrulline.[33] We split this reaction cascade into two parts and represented them with two differential equations: we designed Eq. (1) for describing the Ca^{2+}/calmodulin binding, and the nNOS Eq. (2) to describe the activation of the nNOS enzyme. The following equations represent the variation of the Calm2C concentration:

$$\frac{dCalm2C(t)}{dt} = -\frac{Calm2C(t)}{\tau_c} + [Ca^{2+}]\delta_{spike}, \tag{1}$$

where δ_{spike} is the delta Dirac for a spike, so it has a value of 1 at the time instant of the incoming spike, 0 otherwise. $[Ca^{2+}]$ is the Ca^{2+} concentration that enters the cell at every spike, chosen as $[Ca^{2+}] = 1$ and τ_c is a time constant describing the decay of Calm2C concentration, $\tau_c = 150$ ms.[20] The activation of the nNOS enzyme is modeled using the following equation:

$$\frac{dnNOS(t)}{dt} = -\frac{nNOS(t)}{\tau_{n1}} + \frac{1}{\tau_{n2}}\left(\frac{Calm2C(t)}{Calm2C(t)+1}\right), \tag{2}$$

where τ_{n1} is the time constant describing the decay of activated nNOS enzymes ($\tau_{n1} = 25$ ms), and τ_{n2} is the rate of activation following $Calm2C(t)$ change ($\tau_{n2} = 200$ ms). The $\frac{1}{\tau_{n2}}\left(\frac{Calm2C(t)}{Calm2C(t)+1}\right)$ term is a sigmoidal-like activation ensuring that the response saturates at high Calm2C levels.[20] We then assumed that the amount of NO produced by a source is proportional to the amount of activated nNOS by a constant A,

$$\frac{d[NO](t)}{dt} = A\frac{dnNOS(t)}{dt}, \tag{3}$$

where $A = 1.35 \times 10^{-9}$ better replicates the equivalent simulations performed with the simulator NEURON[31] used as reference.

b. Diffusion equation. To model NO diffusion, we used the heat diffusion equation, where the solution is the NO concentration $[NO](\mathbf{x}, t)$, in $\mathbf{x} = (x, y, z)$ at time t,

$$\frac{\partial[NO](\mathbf{x},t)}{\partial t} = D\nabla^2[NO](\mathbf{x},t) - \lambda[NO](\mathbf{x},t) + S(\mathbf{x},t). \tag{4}$$

Here, D is the diffusion coefficient, which is assumed as a constant scalar, thanks to the low molecular weight and non-polarity of NO, allowing it to diffuse isotropically through the tissue. As reported in Wood *et al.*, we used a diffusion coefficient of 8.48×10^{-10} m^2/s. $\lambda[NO](\mathbf{x}, t)$ is the inactivation term. It represents a first-order reaction that governs the NO consumption in the brain tissue,[4] and it is defined by a rate constant of (λ). This inactivation term can be seen as a simple global loss function that allows us to consider all background reactions involving the NO, i.e., with oxygen species and metals as well as with the *Heam* group of target sGC proteins. Many researchers tried to estimate λ experimentally, both through direct NO measurement and measuring the concentration of other molecules present in its biochemical cascade,[15,19,34] and in the end, we decided to choose a $\lambda = 150\,\mathrm{s}^{-1}$,[15] which make us consider it as a short-lived molecule with a half-life of 4.6 ms, meaning its effects are brief and localized. $S(\mathbf{x}, t)$ is a function describing the dynamics and location of NO sources. In order to solve the NO Eq. (4), we adopt some simplification on the geometry of the problem. First of all, we model each source of NO as a point source, from which the NO diffuses uniformly in all directions. We compute $[NO]$ with respect to the distance r from the source,

not to **x** (3D Cartesian coordinates). This means that the source will have a fixed location in $r = 0$, and it will be described by just its evolution in time, hence $S(t)$. To represent the action of multiple sources, we will simply sum each of their contributions with respect to a given point of observation.

We computed the solution of Eq. (4) by using Green's function, which is an impulse response of an inhomogeneous linear differential operator, defined in a domain with specified initial boundary conditions. In our case, due to the rapid decay in the NO concentration (high inactivation rate), we can assume a finite domain with the boundary condition being $[NO](r,t) \approx 0$ and as initial value, $[NO](r,0) = 0$.[35] The solution for Eq. (4) is then given by the convolution of G, kernel related to Green's function, and $S(t)$, which, in our case is

$$S(t) = \frac{\partial [NO](r,t)}{\partial t} - D\nabla^2 [NO](r,t) + \lambda [NO](r,t). \tag{5}$$

B. NO-dependent plasticity model

1. Cerebellar-inspired spiking neural network

First of all, we employ the cerebellar-inspired SNN developed by Geminiani *et al.,* illustrated in Fig. 6(a). Each population is modeled with point neuron models. In particular, the mossy fibers (*mf*s) and the Glomeruli (Glom) are represented with "*parrot*" neurons, reporting in the output the input signal they receive. The Golgi cells (GoCs), the granule cells (GrCs), the stellate and basket cells (MLIs), and the PC are all represented with the extended-generalized leaky integrate-and-fire (E-GLIF) model, which allows keeping the main electroresponsive features of neurons, while reducing the computational load of simulations.[36] The inferior olivary nuclei (IOs) are modeled as a conductance-based leaky integrate-and-fire neuron. The neuron parameters (reported in supplementary material Table 1) have been tuned for each population model in previous studies,[24] as well as all the connection parameters of the network (supplementary material Table 2). For the sake of simplicity, the neural connections are modeled with a static conductance-based synapse model, with delays extracted from literature and synaptic weights tuned to mirror the resting physiological firing rates observed in mice, in Ref. 24. Only the *pf*-PC synapses exert plasticity and follow an *ad hoc* supervised STDP rule, where LTD is driven by the *cf*s teaching signal.[28]

2. nNOS placement on the Purkinje cell dendritic tree

To reconstruct the geometrical arrangement of nNOS, we consider the synapse density on a single PC dendritic tree area. With an average of approximately 1500 active synapses and a mean dendritic tree area of $3 \times 10^4\ \mu m^2$, we adopt a density of $0.05\ \frac{synapses}{\mu m^2}$.[23] For precise placement of the parallel fiber *pf*-PC synapses, we adhere to the geometrical rule for *pf*-PC connections proposed by the Brain Scaffold Builder (BSB) tool,[23] and then we derive the synapse IDs from the generated GrC-PC connection matrix. Each nNOS is assigned to a geometrical point corresponding to a synaptic bouton on the respective PC dendritic tree, ensuring a unique association between each *pf*-PC synapse and its corresponding nNOS. The coordinates of the geometrical points associated with nNOS are determined as illustrated in Fig. 6(c). The x coordinate aligns with that of the corresponding GrC,

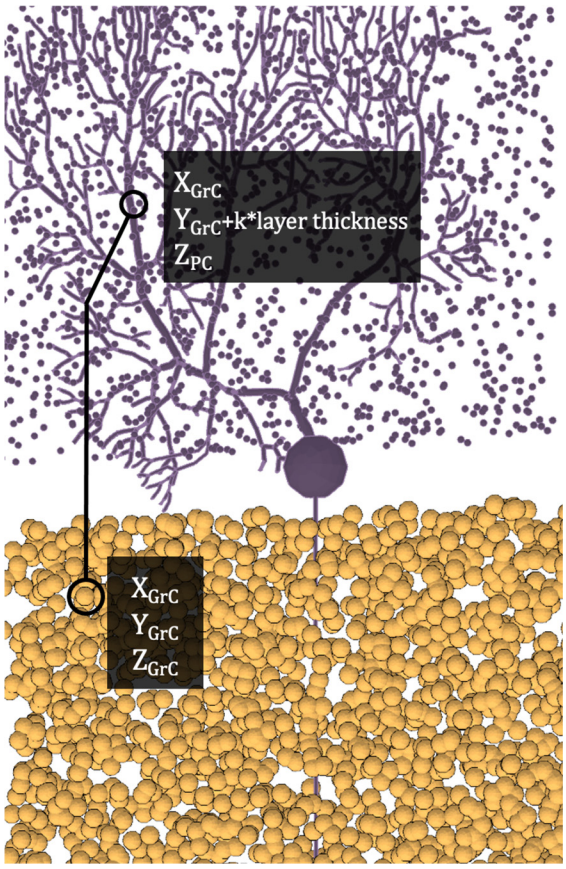

FIG. 6. nNOS placement in PC dendritic tree: nNOS placement is based on the relative connected GrC (yellow) and PC (purple) location in the cerebellar microcircuit volume. Thus, the nNOS coordinates depend on Grc and PC ones as $x_{nNOS} = x_{GrC}, y_{nNOS} = y_{GrC} + k * layer\ thickness, z_{nNOS} = z_{PC}$.

as its ascending axon bifurcates perpendicularly in the molecular layer, crossing the PC dendritic tree. The y coordinate is proportional to the depth of the corresponding GrC in the granular layer. Finally, the z coordinate represents the position within the PC dendritic plane.

3. NO-dependent STDP at pf-PC synapse

The synaptic weights of each *pf*-PC connection evolve following the STDP rule for LTD in and for LTP present in Ref. 28. The plasticity rule is based on the observation that *pf* stimulation coupled with *cf.* activation (teaching signal) triggers LTD at synapses between *pf*s and PCs receiving the *cf* signal, while *pf* stimulation alone causes LTP. We modified this learning rule to include NO-dependent plasticity. To each synapse, we assign a $[NO]$ value computed by summing the diffused concentration from its nNOS and the neighboring ones in a maximum range of 15 μm. This constraint has been chosen in accordance with *Garthwaite*. In this way, we can reduce the computational load at the level of the single source by restricting the diffusion within 15 radius from the source.[4] To model the experimental findings regarding the plasticity enabler role of NO molecule (see Sec. I C), we compute G_{NO}, a sigmoid function that depends on the $[NO]$ and

ranges from 0 to 1 [see Eq. (6)], as an additional gain factor that modulates the learning rate as seen in the following equations:

$$meta_p: G_{NO} = sig\left(\frac{x - [NO]_{thr}}{a}\right) \rightarrow \text{where} [NO]_{thr} = 100\text{pM and } a = 5\,\text{pM}, \tag{6}$$

$$LTD_{\Delta w_i}: \begin{cases} \Delta w_i = G_{NO} \cdot A_{minus} \int_{-\text{inf}}^{t_{cf_{spike}}} k(t_{cf_{spike}} - t) h(t)_{pf_i} dt, \\ k(t) = e^{-\left(\frac{t - t_0}{\tau}\right)} \sin\left(2\left(\frac{t - t_0}{\tau}\right)\right)^{20}, \\ h(t) = \begin{cases} 1, \rightarrow \text{if } pf_i \text{ is active at time t}, \\ 0, \rightarrow \text{otherwise}. \end{cases} \end{cases} \tag{7}$$

$$LTP_{\Delta w_i}: \Delta w_i = G_{NO} \cdot A_{plus} \rightarrow \text{if } pf_i \text{ is active without a } cf \text{ stimulus}. \tag{8}$$

Here, we have two separate mechanisms for LTD and LTP. LTD activated in the *pf*-PC synapses depending on two conditions: (i) activation of pf_i at time t [$h(t) = 1$] and (ii) activation of *cf* connected to the PC at time $t_{cf_{spike}}$. The Δw_i is then calculated by the integration of the STDP kernel [$k(t)$] that depends on both t and $t_{cf_{spike}}$. The integral is then multiplied for A_{minus}, the depression gain ($A_{minus} = -8 \times 10^{-4}$), and G_{NO}. On the other hand, LTP is activated at each pf_i, without a *cf* stimuli, by multiplying A_{plus}, the potentiation gain ($A_{plus} = -1 \times 10^{-4}$), and G_{NO}. In NEST, the device to transmit the teaching signal to the synapses is called *volume transmitter*. In the original implementation,[28] we find a single volume transmitter device for each PC that does not have any physical properties, and each connection would update its weight upon *pf* and *cf* activation in the same time window. When introducing the NO contribution, we have to take into account an additional constraint in the connections' weight update: the relative distances of the synapses. In order to do so, we needed to assign spatial information to the synapses, thus to the volume transmitter devices, which in this case would be associated with each synapse of each PC. Because of this modification with respect to the original network, we had to re-tune the A_plus and A_minus in order to achieve the same learning curves as in Geminiani *et al.* We used a grid-searching algorithm to explore the combination of A_{plus} and A_{minus} (supplementary material Fig. 1). As an index to determine the parameters to select, we used the difference in the firing rate of the PCs pre- and post-learning. By exploring the combination of A_{plus} and A_{minus} values around the one reported by Geminiani *et al.*, we aimed at a depression of 20 Hz in the response of the PCs, evaluated in the interval where the conditioned response should be elicited, i.e., between 100 and 50 ms before the US. The LTP and LTD parameters (A_{plus} and A_{minus}) for *pf*-PC plasticity when NO is enabled have been adapted to match the PC SDF changes observed in the control case (i.e., without NO).

4. Co-simulation NEST and NODS

To test the role of NO in *pf*-PC synapse plasticity, we developed a simulation algorithm that first builds the SNN based on the BSB tool reconstruction and then simulates the network activity following the given inputs, all in NEST simulator,[29] a widely used framework that focuses on the dynamics, size, and structure of neural systems. Given that NO is produced pre-synaptically at the *pf* level, following GrCs activity, we record for each 1 ms of simulation the incoming spikes for each GrC, and we use the spike times for the production equations [Eqs. (1) and (2)] of the paired nNOS in the PC dendritic trees. After the production of NO, we evaluate the diffusion of it and sum in each synapse the NO concentration at each time instant.

5. Compare standard and NO-dependent STDP

To test the NO role as an enabler for plasticity, we run two sets of five simulations, 30 trials each, where only background noise is delivered to the *mf* input of the network. Here, we compare the standard STPD rule that defines *pf*-PC weight updates in the cerebellar network. In the second ten simulations, instead, the NO-dependent STDP rule controls *pf*-PC weight updates. Then, in order to test the contribution of NO in the learning process of the cerebellum, we first reproduced the EBCC protocol proposed in Geminiani *et al.* for the physiological network, and we compared the network performance under the same conditions, but modifying the learning rule to account for NO diffusion. In the proposed EBCC protocol, a conditioned stimulus (CS) is conveyed by a subset of *mf*s, each receiving a non-recurrent 40 Hz spike train for 280 ms. The teaching signal, the unconditioned stimulus (US), is a 500 Hz burst delivered to IOs for 30 ms. The CS and US stimuli co-terminate after 380 ms after the start of each trial [Fig. 6(b)]. All *mf*s receive a background noise, modeled with a Poisson generator. We tested three different background noise values (0, 4, and 8 Hz), and then we compared the standard and NO plasticity. To better evaluate the learning outcome of NO-dependent plasticity, we split both the PC and the DCN populations into two subpopulations each. The PC population was divided by calculating for each PC the amount of *pf*-PC synapses conveying the CS and selecting as PC-CS (PC receiving mostly CS) the ones that had more of the 30% of the CS-synapses and PC-noise (PC receiving mostly noise stimuli) with an amount lower than 30%. Furthermore, following the same concept, we calculated the number of PC-CS connected to each DCN, and we divided the population between those receiving an equal or higher number of average of PC-CS (DCN-CS) and the ones receiving less than the mean value. First, to assess firing modulation, we computed the SDF as the convolution of each cell's spikes in every trial, with a Gaussian kernel of 20 ms for all the subpopulations of PCs and DCNs.[37] SDFs of the population were then computed by averaging SDFs of individual cells. To quantify learning in terms of neural activity, an index of SDF-change was computed in the expected CR time window, between 250 and 300 ms, and over the trial baseline window, between 150 and 200 ms from the CS onset. The SDF-change index is computed for each trial as the SDF mean in the time window of interest subtracted by the SDF mean in the same time window of the first trial. Finally, we computed the CR% of each simulation by evaluating trial by trial the percentage of SDF values of DCNs over the threshold in both the CR window and baseline window. For each trial, we identified a CR, if the SDF values were over the threshold for at least 75% in the CR window and below 75% in the baseline window. To calculate the final CR%, we applied a moving average considering ten trials, with a left zero-padding, and then we mediated through all the simulations. We chose to calculate the CR% with this strategy as done by Geminiani *et al.* in order to quantify the amount of learning exerted by the cerebellar SNN during the EBCC protocol.

SUPPLEMENTARY MATERIAL

See the supplementary material for neuron and synapses parameters, comparison with data of Garthwaite *et al.*, details of grid search for the A_{plus} and A_{minus} parameters, and representation of NO diffusion during EBCC simulations. It also contains the NO concentration traces during EBCC simulation and all the SDFs for PC and DCN subpopulations.

ACKNOWLEDGMENTS

The work of A.A., A.P., B.G., and C.A.S. in this research is also supported by the Horizon Europe Program for Research and Innovation under Grant No. 101147319 (EBRAINS 2.0).

The work of A.M.T. was supported by a research grant (CEoI 4-Rodent microcircuits: RisingNet Whole-bRaIn rodent SpikING neural NETworks) from the European Union's Horizon 2020 Framework Programme for Research and Innovation under the Specific Grant Agreement No. 945539 (Human Brain Project SGA3). The simulations in NEURON were implemented by Stefano Masoli, Department of Brain and Behavioral Sciences, Universitá di Pavia, Pavia, Italy.

Funding

The project "EBRAINS-Italy (European Brain ReseArch INfrastructureS-Italy)," granted by the Italian National Recovery and Resilience Plan (NRRP), M4C2, and funded by the European Union—NextGenerationEU (Project IR0000011, CUP B51E22000150006, "EBRAINS-Italy") to A.A. and A.P. supported this work and fully covered the publication fees of this article.

AUTHOR DECLARATIONS

Conflict of Interest

The authors have no conflicts to disclose.

Ethics Approval

Ethics approval is not required.

Author Contributions

Alessandra Maria Trapani: Conceptualization (lead); Data curation (lead); Formal analysis (lead); Investigation (lead); Methodology (lead); Software (lead); Validation (lead); Visualization (equal); Writing – original draft (lead); Writing – review & editing (lead). **Carlo Andrea Sartori:** Conceptualization (equal); Data curation (equal); Formal analysis (equal); Investigation (equal); Methodology (equal); Software (equal); Visualization (equal); Writing – original draft (equal); Writing – review & editing (equal). **Benedetta Gambosi:** Conceptualization (equal); Data curation (equal); Formal analysis (equal); Investigation (equal); Methodology (equal); Software (lead); Validation (equal); Visualization (supporting); Writing – original draft (equal); Writing – review & editing (supporting). **Alessandra Pedrocchi:** Conceptualization (equal); Funding acquisition (lead); Investigation (equal); Supervision (equal); Writing – original draft (supporting); Writing – review & editing (supporting). **Alberto Antonietti:** Conceptualization (equal); Funding acquisition (equal); Investigation (equal); Project administration (equal); Supervision (equal); Writing – original draft (equal); Writing – review & editing (equal).

DATA AVAILABILITY

The data that support the findings of this study are openly available in GitHub at https://github.com/near-nes/NODS, Ref. 38.

REFERENCES

[1]J. O. Lundberg and E. Weitzberg, "Nitric oxide signaling in health and disease," Cell **185**, 2853–2878 (2022).
[2]P. Picón-Pagès, J. Garcia-Buendia, and F. J. Muñoz, "Functions and dysfunctions of nitric oxide in brain," Biochim. Biophys. Acta **1865**, 1949–1967 (2019).
[3]D. E. Koshland, "The molecule of the year," Science **258**, 1861–1861 (1992).
[4]J. Garthwaite, "From synaptically localized to volume transmission by nitric oxide," J. Physiol. **594**, 9–18 (2016).
[5]N. Hardingham, J. Dachtler, and K. Fox, "The role of nitric oxide in presynaptic plasticity and homeostasis," Front. Cell. Neurosci. **7**, 1–19 (2013).
[6]A. Haghikia, E. Mergia, A. Friebe, U. T. Eysel, D. Koesling, and T. Mittmann, "Long-term potentiation in the visual cortex requires both nitric oxide receptor guanylyl cyclases," J. Neurosci. **27**, 818–823 (2007).
[7]X. Liu and J. L. Zweier, "Application of electrode methods in studies of nitric oxide metabolism and diffusion kinetics," J. Electroanal. Chem. **688**, 32–39 (2013).
[8]N. Hardingham and K. Fox, "The role of nitric oxide and GluR1 in presynaptic and postsynaptic components of neocortical potentiation," J. Neurosci. **26**, 7395 (2006).
[9]J. Dachtler, N. R. Hardingham, and K. Fox, "The role of nitric oxide synthase in cortical plasticity is sex specific," J. Neurosci. **32**, 14994–14999 (2012).
[10]K. G. Phillips, N. R. Hardingham, and K. Fox, "Postsynaptic action potentials are required for nitric-oxide-dependent long-term potentiation in CA1 neurons of adult GluR1 knock-out and wild-type mice," J. Neurosci. **28**, 14031–14041 (2008).
[11]S. Yang and C. L. Cox, "Modulation of inhibitory activity by nitric oxide in the thalamus," J. Neurophysiol. **97**, 3386–3395 (2007).
[12]V. Lev-Ram, S. T. Wong, D. R. Storm, and R. Y. Tsien, "A new form of cerebellar long-term potentiation is postsynaptic and depends on nitric oxide but not cAMP," Proc. Natl. Acad. Sci. U. S. A. **99**, 8389–8393 (2002).
[13]D.-J. Wang, L.-D. Su, Y.-N. Wang, D. Yang, C.-L. Sun, L. Zhou, X.-X. Wang, and Y. Shen, "Long-term potentiation at cerebellar parallel fiber-Purkinje cell synapses requires presynaptic and postsynaptic signaling cascades," J. Neurosci. **34**, 2355–2364 (2014).
[14]M. Kono, W. Kakegawa, K. Yoshida, and M. Yuzaki, "Interneuronal NMDA receptors regulate long-term depression and motor learning in the cerebellum," J. Physiol. **597**, 903–920 (2019).
[15]K. C. Wood, A. M. Batchelor, K. Bartus, K. L. Harris, G. Garthwaite, J. Vernon, and J. Garthwaite, "Picomolar nitric oxide signals from central neurons recorded using ultrasensitive detector cells," J. Biol. Chem. **286**, 43172–43181 (2011).
[16]A. Maffei, F. Prestori, K. Shibuki, P. Rossi, V. Taglietti, and E. D'Angelo, "NO enhances presynaptic currents during cerebellar mossy fiber-granule cell LTP," J. Neurophysiol. **90**, 2478–2483 (2003).
[17]G. Bouvier, D. Higgins, M. Spolidoro, D. Carrel, B. Mathieu, C. Léna, S. Dieudonné, B. Barbour, N. Brunel, and M. Casado, "Burst-dependent bidirectional plasticity in the cerebellum is driven by presynaptic NMDA receptors," Cell Rep. **15**, 104–116 (2016).
[18]V. Lev-Ram, T. Jiang, and J. Wood, "Synergies and coincidence requirements between NO, cGMP, and Ca^{2+} in the induction of cerebellar long-term depression," Neuron **18**, 1025 (1997).
[19]R. M. Santos, C. F. Lourenço, F. Pomerleau, P. Huettl, G. A. Gerhardt, J. Laranjinha, and R. M. Barbosa, "Brain nitric oxide inactivation is governed by the vasculature," Antioxid. Redox Signaling **14**, 1011–1021 (2011).
[20]Y. Sweeney, J. Hellgren Kotaleski, and M. H. Hennig, "A diffusive homeostatic signal maintains neural heterogeneity and responsiveness in cortical networks," PLoS Comput. Biol. **11**, e1004389 (2015).
[21]H. Ogasawara, T. Doi, K. Doya, and M. Kawato, "Nitric oxide regulates input specificity of long-term depression and context dependence of cerebellar learning," PLoS Comput. Biol. **3**, e179 (2007).

[22]K. Safaryan, R. Maex, N. Davey, R. Adams, and V. Steuber, "Nonspecific synaptic plasticity improves the recognition of sparse patterns degraded by local noise," Sci. Rep. **7**, 46550 (2017).
[23]R. De Schepper, A. Geminiani, S. Masoli, M. F. Rizza, A. Antonietti, C. Casellato, and E. DAngelo, "Model simulations unveil the structure-function-dynamics relationship of the cerebellar cortical microcircuit," Commun. Biol. **5**, 1240 (2022).
[24]A. Geminiani, A. Mockevicius, E. DAngelo, and C. Casellato, "Cerebellum involvement in dystonia during associative motor learning: Insights from a data-driven spiking network model," Front. Syst. Neurosci. **16**, 919761 (2022).
[25]M. Manto, J. M. Bower, A. B. Conforto, J. M. Delgado-García, S. N. F. da Guarda, M. Gerwig, C. Habas, N. Hagura, R. B. Ivry, P. Mariën, M. Molinari, E. Naito, D. A. Nowak, N. Oulad Ben Taib, D. Pelisson, C. D. Tesche, C. Tilikete, and D. Timmann, "Consensus Paper: Roles of the cerebellum in motor control—The diversity of ideas on cerebellar involvement in movement," Cerebellum **11**, 457–487 (2012).
[26]J. H. Freeman, "Cerebellar learning mechanisms," Brain Res. **1621**, 260–269 (2015).
[27]K. Takehara-Nishiuchi, "The anatomy and physiology of eyeblink classical conditioning," in *Behavioral Neuroscience of Learning and Memory*, Series Title: Current Topics in Behavioral Neurosciences Vol. 37, edited by R. E. Clark and S. J. Martin (Springer International Publishing, Cham, 2016), pp. 297–323.
[28]A. Antonietti, C. Casellato, J. A. Garrido, N. R. Luque, F. Naveros, E. Ros, E. DAngelo, and A. Pedrocchi, "Spiking neural network with distributed plasticity reproduces cerebellar learning in eye blink conditioning paradigms," IEEE Trans. Biomed. Eng. **63**, 210–219 (2016).
[29]M.-O. Gewaltig and M. Diesmann, "NEST (neural simulation tool)," Scholarpedia **2**, 1430 (2007).
[30]M. Stimberg, R. Brette, and D. F. Goodman, "Brian 2, an intuitive and efficient neural simulator," eLife **8**, e47314 (2019).
[31]P. Kumbhar, M. Hines, J. Fouriaux, A. Ovcharenko, J. King, F. Delalondre, and F. Schürmann, "CoreNEURON: An optimized compute engine for the NEURON simulator," Front. Neuroinf. **13**, 63 (2019).
[32]J. A. Garrido, E. Ros, and E. D'Angelo, "Distributed synaptic plasticity controls spike-timing: Predictions from a cerebellar computational model," BMC Neurosci. **14**, P81 (2013).
[33]C. N. Hall and J. Garthwaite, "What is the real physiological NO concentration in vivo?," Nitric Oxide **21**, 92–103 (2009).
[34]J. Laranjinha, R. M. Santos, C. F. Lourenço, A. Ledo, and R. M. Barbosa, "Nitric oxide signaling in the brain: Translation of dynamics into respiration control and neurovascular coupling," Ann. N.Y. Acad. Sci. **1259**, 10–18 (2012).
[35]E. J. Poirier and D. R. Poirier, "Conduction of heat in solids," in *Minerals, Metals and Materials Series* (Springer International Publishing, 2016), pp. 158–188.
[36]A. Geminiani, C. Casellato, F. Locatelli, F. Prestori, A. Pedrocchi, and E. D'Angelo, "Complex dynamics in simplified neuronal models: Reproducing Golgi cell electroresponsiveness," Front. Neuroinf. **12**, 88 (2018).
[37]P. Dayan and L. F. Abbott, *Theoretical Neuroscience: Computational and Mathematical Modeling of Neural Systems* (MIT Press, 2001).
[38]See https://github.com/near-nes/NODS for "GitHub."